Serendipities in the Solar System and Beyond – Celebrating Prof. Wing-Huen Ip's 70th Birthday
ASP Conference Series, Vol. 513
C. M. Ko, P. C. Yu and C. K. Chang, eds.

Determinations of Shape and Photometric Phase Function of Selected Asteroids

Xiaobin Wang[1,2,5] and Karri Muninonen [3,4]

[1]*Yunnan Observatories,CAS, Kunming 650216, China;*wangxb@ynao.ac.cn

[2]*Key Laboratory for the strucure and evoltion of celestial objects, CAS, Kunming 650216, China*

[3]*Department of Physics, University of Helsinki,P.O.Box 64, FI-000014 Helsinki,Finland*

[4]*Finnish Geospatial Research Institute, P.O.Box 15, FI-02431 Masala,Finland*

[5]*University of Chinese Academy of Sciences, China*

Abstract. The ground-based photometric observations of asteroids still is the main source to understand their basic physical properties, even though some space mission and space-based instruments have been applied in physical studies of asteroids. Owing to developments on scattering theories and 3D shape models of asteroid, we can carry out determination for basic physical parameters of asteroids from the photometric data. Here, we present photometric observations for some selected asteroids and light inversion results for these asteroids. In detail, they are: (1) To determine photometric phase functions of asteroids (107)Camilla and (106) Dione considering an ellipsoid shape and a cellinoid shape respectively; and (2) To inverse convex shape of main-belt slow rotating asteroids (168) Sibylla and (346)Hermentaria and a near Earth asteroid (3200) Phaethon. Based on derived photometric phase functions, the geometric albedo, and even rough taxonomic classification of asteroids are inferred. With the virtual photometry Monta Carlo method, the uncertainties of spin parameters of selected asteroids were compared.

1. Introduction

The earliest photometric observations for asteroids made with photometers could back to 1887 (Müller 1893), and the light variation with the solar phase angle and another a variation in a period of several hours had been noted at that time (1911 Harvard College Observatory circular 169,). As everyone knows that the brightness of asteroid is the fraction of solar light reflected by asteroid's surface illuminated and visible. For a spheroid asteroid, the change of distances from the Sun and observer to asteroid, and the change of observational geometry cause the change of brightness. For a non-spheroid asteroid, an additional variation in period of several hours will occur because of the change of the apparent cross-section during its rotating. Sometimes, inhomogeneous material over asteroid surface also can give a light variation in the spin period, which may be identified by color-index or spectroscopic observation over the surface of asteroid.

That the variation of asteroid's integrated brightness vs solar phase angle is called as photometric phase function /or phase curve of asteroid. The opposition effect is a significant increase in brightness nearby small phase angle, which is firstly found and explained by Seeliger (1887) on Saturn's rings observations. Later, the photometric phase curves of more and more asteroids were obtained using ground-based telescopes. Several brightness models of small atmosphereless bodies in the solar system were developed by Hapke (1963), Hapke (2012), Irvine (1966), Bobrov (1970),Lumme (1970) Lumme & Bowell (1981a), Lumme & Bowell (1981b),Lumme et al. (1987), Esposito (1979), Shkuratov (1985), Muinonen et.al (1989), and Mishchenko & Dlugach (1993).

Among those existed brightness models, Hapke model and Lumme & Bowell model were widely used. The two models considered effects of microstructure, multiple scattering and large-scale roughness. Theoretically, one can infer regolith optical properties of asteroids through geometric albedo and phase function if given disk-resolved and high precision disk-integrated photometric data in a large solar phase angle range.

At present, only a few asteroids (e.g. targets of space missions: Ida, Eros, Mathilde, Itokawa, Stains, Lutatia, Vesta and Ceres) had been accurately determined their surface physical parameters using either Hapke model or Lumme& Bowell model for having disk-resolved and high precision disk-integrated photometric data in a wider solar phase angle. But for most asteroids, only ground-based photometric data are available. The limited range of solar phase angles of ground-based observation and unknown irregular shape are main obstacles in obtaining unambiguous values for the surface physical parameters.

At the early stage of determination of asteroids' phase function, approximate expressions for integrated phase function and geometric albedo were used assuming a spherical shape of asteroid. For a main-belt asteroid, it takes long time period(several apparitions) to get enough photometric data in a large range of solar phase angle. As a result of irregular shape of asteroid, the varied apparent cross-section area due to the change of aspect angle in different apparitions brings additional light variation besides the variation vs solar phase angle. To overcome such an influence, a mean magnitude of lightcurve over its spin period or the magnitude of a specific feature (e.g. maxima or minimum) of light curves were taken during the determination of asteroids' phase function .

Nowadays, more and more photometric data span long time period and developments on scattering theory and shape model of asteroids provide us opportunities to determine shape and phase function of asteroids accurately. Hundreds of asteroid were determined their 3D shape from the integrated and/or disk-resolved photometric data obtained by space- and ground-based instruments, stellar occultation timing, and radar doppler data. The shape determination of asteroids' is becoming a fundamental work for figuring out surface physical properties(including phase function property) and providing scientific basis for spacecraft observation in future. Having accurate shape and spin parameters for an asteroid, the light incidence and emergence angles to an elemental facet on the surface of irregular asteroids can be computed accurately, and then the corresponding surface physical parameters and phase function can be determined more accurately than before. So, section 2 gives simple introduce on often using scattering laws in lightcurve analysis of asteroid. Section 3 presents determination of three-parameter phase function HG_1G_2 (Muinonen et.al 2010) for asteroid (107) Camilla and (106) Dione based on ellipsoid and cellinoid shape models. Section 4 reports the convex inversion for selected slow rotating main-belt asteroids and a near earth asteroid. Last

section is simple discussions on derived phase function and convex shape of selected asteroids.

2. Brightness models of asteroids

Brightness of asteroid is scattered radiance from its upper surface by incident irradiance. For an elemental facet of a normal vector $\vec{n}$ on the asteroid surface, observed intensity can be expressed as the product of incident radiance J and the bidirectional reflectance $r(i, e, \alpha)$: $I(i, e, \alpha) = J * r(i, e, \alpha)$. α is solar phase angle. i and e are the light incidence and emergence angles of a facet. Usually, another two quantities μ and μ_0, cosine functions of incidence and emergence angles are used in photometric model of asteroid. Brightness of a elemental facet illuminated by solar light can be computed given a bidirectional reflectance $r(i, e, \alpha)$.

2.1. Often used scattering laws

There existed several often used empirical models for bidirectional reflectance in planetary photometry: Lambert law (Lambert 1760), Lommel-Seeliger law (Seeliger 1887), Minnaert law (Minnaert 1941), Lunar-Lambert law (Buratti&Veverk 1985), Hapker model (Hapke 2012) and Bowell-Lumme models (Bowell&Lumme 1979).

The Lambert law (Equation (1)) describes bright surfaces (geometric albedo close to or greater than unity) well, in which an anisotropic single particles scattering $p(\alpha)$ is considered. For an isotropic single particle scattering case, $P(\alpha) = 1$. A_L is Lambertian albedo.

$$r_L(\mu, \mu_0, \alpha) = \frac{1}{\pi} A_L \mu_0 * P(\alpha) \tag{1}$$

Lommel-Seeliger law, as a first approximation to diffuse reflection, describes low-reflectance surface(geometric albedo less than 0.2) well, e.g. C-, D-, P-types asteroids.

$$r_{LS}(\mu, \mu_0, \alpha) = A_{LS} \frac{\mu_0}{\mu_0 + \mu} p(\alpha) \tag{2}$$

Minnaert law, a generalization form of Lambert law, can describe variety surfaces over a limited range of angles.

Lunar-Lambert model actually is the combination of a Lambert and Lommel-Seeliger law with a weight factor. This model work well to those surfaces with higher albedo, e.g. S-type and V- and E-types asteroids.

Lumme-Bowell and Hapke laws/or brightness models are actually the approximate solution for radiative transfer from a rough, particulate surface. In which several physical processes: single scattering, multiple scattering, shadow-hiding opposition effect(SHOE) and /or coherent backscattering opposition effect (CBOE) were involved. Also, effects of anisotropic scattering of single-particle and roughness of surface on reflectance were considered in both models. The detail formula can refer the equation (15) and (24) in the Bowell's paper (Bowell et al. 1989).

In Lumme-Bowell and Hapke brightness models, the surface physical parameters–single-scattering albedo, roughness parameter, amplitude and width of opposition effect, volume density of the regolith and asymmetry parameter g, were involved. We can derive the reliable analysis result for surface physical parameters based on Hapke

model or Bowell-Lumme model if having disk-resolved photometric data in a large range of illuminated and viewing geometry and /or high precise integrated photometric data covered an opposition surge and extended to large solar phase angle. That's the reason that only a few asteroid, Ceres, Itokawa, steins, Lutetia, Annefrank, and Vesta were determined their surface physical parameters since they were visited by space mission.

2.2. Integrated brightness models

In order to understand the surface property of more asteroids, the integrated bidirectional reflectance / or 'disk-integrated phase function' were actually used, which is an integration of certain a reflectance over the hemispherical surface. Li (2015) lists disk-integrated phase functions corresponding to Lambert law, Lommel-Seeliger law, Lunar-Lambert law and Hapke law. Assuming a spherical shape of asteroid, Lumme & Bowell gave the expression for the disk-integrated phase function (see Equation (7) in Lumme & Bowell (1981a)). Later, Bowell et al. (Bowell et al. 1989) proposed an approximations for their disk-integrated phase function by adopted mean values for roughness $\rho = 1.17$, volume density $D = 0.37$, and asymmetry parameter $g = -0.1$. In the approximate disk-integrated phase function (following equation), two unknown parameter Q and $m(0^\circ)$ are needed to be estimated. The multiple scattering factor Q is the function of the single scattering and asymmetry factor of asteroid's surface, and the absolute magnitude $m(0^\circ)$ is the function of size and geometric albedo of asteroid.

$$\begin{aligned} &m(\alpha) = m(0^\circ) - 2.5\log_{10}[(1-Q)\phi_1(\alpha) + Q\phi_M(\alpha)] \\ &\phi_1(\alpha) = exp(3.343(\tan(\tfrac{\alpha}{2}))^{0.632}) \\ &\phi_M(\alpha) = \tfrac{1}{\pi}[\sin(\alpha) + (\pi-\alpha)\cos(\alpha)] \end{aligned} \tag{3}$$

That is the proto equation of the HG magnitude system, which was adopted as the standard magnitude of asteroids at the IAU General Assembly in 1985. G is slope parameter, H is the absolute magnitude.

$$\begin{aligned} &m(\alpha) = H(0^\circ) - 2.5\log_{10}[(1-G)\phi_1(\alpha) + G\phi_2(\alpha)] \\ &\phi_i(\alpha) = e^{-A_i(\tan(\frac{\alpha}{2})^{B_i})}, i = 1,2 \\ &A_1 = 3.33, B_1 = 0.63 \\ &A_2 = 1.87, B_2 = 1.22 \end{aligned} \tag{4}$$

Recently, a three-parameter photometric phase function model HG_1G_2 system was proposed by Muinonen et.al (2010). This novel model could improve the fitting to the phase curves of high-albedo and low-albedo asteroids compared to that of HG phase function, and was officially adopted as an new magnitude system of asteroid in the 28th IAU General Assembly.

$$\begin{aligned} &m_v(\alpha) = H(0) - 2.5log_{10}(G_1 * \phi_1(\alpha) + G_2 * \phi_2(\alpha) + (1-G_1-G_2) * \phi_3(\alpha)) \\ &\phi_1(\alpha) = 1 - \frac{6\alpha}{\pi} \\ &\phi_2(\alpha) = 1 - \frac{9\alpha}{5\pi} \\ &\phi_3(\alpha) = exp(-4\pi\tan^{\frac{2}{3}}\tfrac{\alpha}{2}) \end{aligned} \tag{5}$$

The 'disk-integrated phase function'(hereafter simply as phase function) is the normalized integrated-brightness of asteroid assuming a spheroid shape. Above formulas cannot be applied to asteroids of non-spherical shape for ignoring the effect of

irregular shape of asteroids. For determining of phase curve for selected asteroids of non-spheroid, we introduced the ellipsoid and cellinoid shape model into the integrated brightness model.

3. Determination of integrated phase function of non-spherical asteroids

Most asteroids are non-spheroid. Medium- and small-size asteroids, thought of the fragmentation of a parent body's caused by collisions have more irregular shape; large asteroids, maybe the remnants of original planetesimals or the gravitational re-accumulated rubble piles show more regular shapes: Spheroid or biaxial and triaxial ellipsoids.

The light variation in one apparition mainly risen from a non-spherical asteroid's rotating. Lightcurves of different apparition can be used to infer the shape and spin status of asteroids. Given the shape and spin parameters of asteroid, the apparent surface of a non-spheroid asteroid at different apparitions /or of different aspect angle can be normalized when we determine its phase function. Sometimes, the simulations for shape, spin parameters and the phase function of asteroid are done simultaneously.

Following, we will present the determination of phase function for selected main-belt asteroids. In brightness models of asteroid, a simply shape model, triaxial ellipsoid and a more complicated shape, cellinoid shape are used to represent asteroid's shape. The brightness model of triaxial ellipsoid shape will be applied in the lightcuves with equal maximum and minima, e.g. case of (107) Camilla (see left panel of Figure 1), and the brightness model of cellinoid shape (Cellino et al. 1989) can be applied in the lightcurves of different maximum and/or minima, like lightcurves of (106) Dione (see Figure 2).

3.1. Phase function of asteroid assuming an ellipsoid shape

For some large asteroids, an ellipsoid shape model is used when we determine their three-parameter phase function HG_1G_2. The bidirectional reflection coefficient r we used is the improved Lommel-seeliger reflectance coefficient (Wilkman et al. 2015).

$$r(\mu, \mu_0, \alpha) = \frac{1}{4}\varpi(\alpha)\frac{1}{\mu + \mu_0} \tag{6}$$

For a spheroid case, the integrated brightness of asteroids is written as follows (Muinonen et al. 2015):

$$\begin{aligned} &L(\overrightarrow{i}, \overrightarrow{e}, \alpha) = \int_{A_+} r(\mu, \mu_0, \alpha) F_0 \mu \mu_0 dA = \tfrac{1}{32}\varpi F_0 P(\alpha)\phi_{LS}(\alpha) \\ &Let: \tfrac{1}{8}\varpi P(\alpha)\phi_{LS}(\alpha) = p * \phi_{HG_1G_2}(\alpha), p = \tfrac{1}{8}\varpi P(0) \\ &Finally, L(\alpha) = \tfrac{1}{4}\pi D^2 p F_0 \phi_{HG_1G_2} \end{aligned} \tag{7}$$

Where $\overrightarrow{i}$ and $\overrightarrow{e}$ are unit vector of light source and observer,respectively in the asteroid-fixed coordinate frame. A_+ donates the illumined and visible surface area; $\phi_{LS}(\alpha)$ is the integrated phase function of Lommel-Seeliger law; ϖ is single particle albedo. $P(\alpha)$ phase function of single particle. Finally, the brightness is function of solar phase angle α, the diameter of asteroid D, and three phase function parameters H, G_1 and G_2.

For an ellipsoid shape case (the principal axes: $a > b > c$), the integrated brightness of asteroid can be written following formula:

$$L(\overrightarrow{i}, \overrightarrow{e}, \alpha) = \frac{1}{4} D^2 \varpi P(\alpha) F_0 \phi_{HG_1G_2}(\alpha) \left(\frac{\phi_{Ellip}(\overrightarrow{i}, \overrightarrow{e}, \alpha)}{\phi_{LS}(\alpha)}\right) \tag{8}$$

In magnitude form:

$$\begin{aligned} V(\alpha) &= H(0^\circ) + G_1\phi_1(\alpha) + G_2\phi_2(\alpha) + (1 - G_1 - G_2)\phi_3(\alpha) + \Delta m \\ \Delta m &= -2.5(\log(\phi_{Ell-LS}(\overrightarrow{i}, \overrightarrow{e}, \alpha) - \log(\phi_{LS}(\alpha)) \end{aligned} \tag{9}$$

D is the diameter of an equivalent spheroid to an ellipsoid ($a * b * c = (D/2)^3$), $\phi_{Ellip}(\overrightarrow{i}, \overrightarrow{e}, \alpha)$ denotes the integrated brightness of Lommel-Seeliger law over a scaled ellipsoid ($a * b * c = 1$) at solar phase angle α. Δm is deviation of the integrated brightness of the scaled ellipsoid from that of an unit spheroid. In the above equation, the spin parameters(longitude and latitude of pole, and spin rate), shape parameters(three semi-major axes, or ratio of semi axes) are contained in Δm, the phase function parameters $(H(0^\circ), G_1, G_2)$ are separated in another part.

The procedure of estimation for unknown parameter actually were carried out in two steps: First step, to find solution of the spin parameters and shape parameters of asteroid from the observed photometric data, and second step, to fit the phase parameters using reduced photometric data from which the variation caused by the non-spherical shape was removed. The calculation for $\phi_{Ellip}(\overrightarrow{i}, \overrightarrow{e}, \alpha)$ used the same formula of equation (13) in paper of Muinonen et al. (2015). In the analysis procedure, a Markov Chain Monte Carlo (MCMC) method was used to derive best values for the unknown parameters.

As an application, the photometric data of asteroid (107) Camilla were analyzed with Lommel-Seeliger ellipsoid model. In all, 20 lightcurves of Camilla obtained from 1981 to 2015 were involved in the photometric inversion. Among those data, new observed magnitudes of target's were transferred into the CMC15 catalog system by the field stars in the images, then they were converted into the standard photometric system by the Equation (2) of Dymock (2009). After first step of simulation, a pole of $(74.1^\circ, 50.2^\circ)$ Camilla was derived with spin period of 4.843928 hour. The ratio of axes of an ellipsoid shape are a/b = 1.409 and b/c = 1.249, respectively. Then the best values for parameters $H(0^\circ)$, G_1 and G_2 are 7.026 mag, 0.489 and 0.259, respectively. The phase function of (107) Camilla is shown in the right panel of Figure 1. For asteroids of approximate biaxial and triaxial ellipsoid shape, the above brightness model simulates the photometric data well, and can give more accurate solution for the phase function parameters.

3.2. Phase function of asteroid assuming a cellinoid shape

For asteroid of more irregular shape, a more complicated shape model, cellinoid (Cellino et al. 1989) was used to represent asteroid's shape, which consists of eight adjacent octants of ellipsoids with six semi-axes$\{a_1, a_2, b_1, b_2, c_1, c_2\}$(see left panel of Figure 3). The integrated brightness of asteroid was computed by summing reflectance radiance by triangular facets illuminated and visible over a cellinoid surface. Correspondingly, the origin of asteroid-fixed equatorial rectangular coordinate is shifted to the mass center of the cellinoid $(\frac{3}{8}(a_1 - a_2), \frac{3}{8}(b_1 - b_2), \frac{3}{8}(c_1 - c_2))$. The bidirectional reflectance

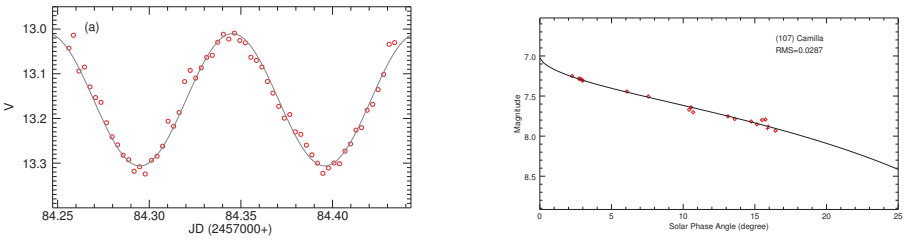

Figure 1. Left: One Lightcurve of (107) Camilla; Right: Phase curve of (107) Camilla.

coefficient used is the combination of Lommel-Seeliger law and Lambert law with a weight factor w. The main difference from Lommel-Seeliger ellipsoid method is the way to calculate $\phi_{cellinoid}(\overrightarrow{i}, \overrightarrow{e}, \alpha)$.

$$\begin{aligned} \phi_{cellinoid}(\overrightarrow{i}, \overrightarrow{e}, \alpha) &= \sum r_{LS-L}(\mu_0, \mu, \alpha) d\sigma \\ r_{LS-L}(\mu, \mu_0, \alpha) &= \frac{1}{4} \varpi P(\alpha) (\frac{\mu_0}{\mu_0 + \mu} + w\mu_0) \end{aligned} \tag{10}$$

The detailed calculation for the area size $d\sigma$ and normal n of each of triangular facets can refer our paper (Wang et al. 2017). In shortly, the spin parameters (λ_p,β_p, $peroid$, ϕ_0), axial ratios of Cellinoid shape($(a/b, b/c, a_1/a, b_1/b, c_1/c)$ and weight factor w were simulated with a MCMC method. Then the phase function parameters (H, G_1, G_2) are subtracted from the reduced magnitude.

Using this brightness model, 26 lightcurves of asteroid (106)Dione obtained at four apparitions were analyzed. At the first step, a pole of $(58°.0, 21°.1)$ with a spin period of 16.2345 hour was derived, the corresponding cellinoid shape are $(a/b = 1.10, b/c = 1.59, a_1/a = 1.65, b_1/b = 0.86, c_1/c = 1.64)$. The observed photometric data (Dots points) in 2004 and 2012 and modeled data (Solid line) are presented in Figure 2. The fitted phase function of (106) Dione is presented with doted line in the right panel of Figure 3. The best values for H, G_1, and G_2 are derived as 7.66 mag, 0.682 and 0.081 respectively.

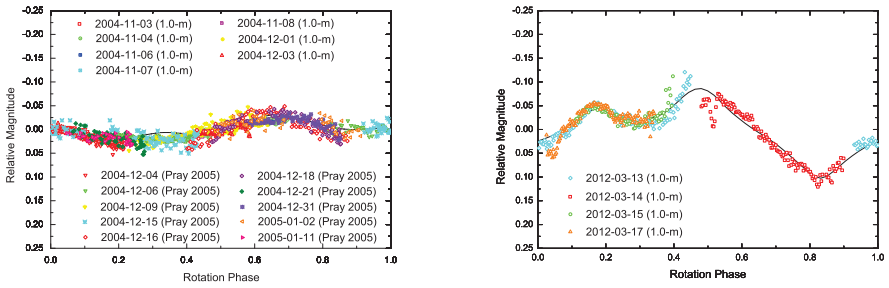

Figure 2. Lightcurves of (106) Dione.

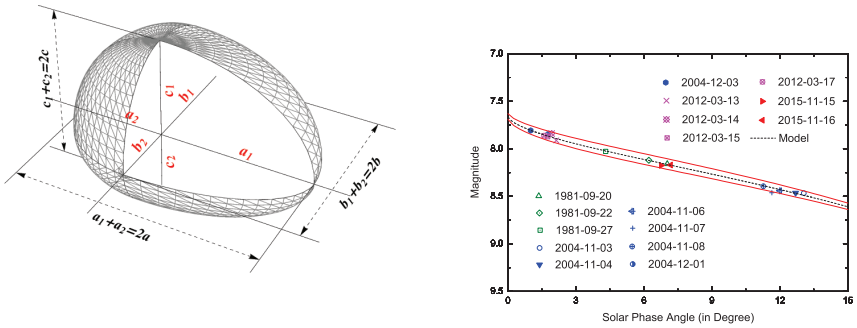

Figure 3. Left: Sketch of a cellinoid shape. Right:Phase function of (106) Dione (Doted line is fitted phase function, red lines represent 1σ uncertainty of fitted phase function).

4. Convex inversion of asteroids

Space-based, adaption and radar observations provided us new and fine appearance for few special asteroids. However, ground-based photometric observation still is the main source for most asteroids to find their shape and surface physical properties. From ground-based integrated photometric data, the convex inversion method (Kaasalainen & Troppa 2001) gives a convex shape which wraps the real shape of asteroid.

4.1. Main-belt slow rotating asteroids

The spin rate of larger asteroids of $125 < D < 200km$ and $D \geq 200km$ show Maxwellian distributions. The non-Maxwellian distribution of slow rotating asteroids with $D < 125km$ implies another mechanism, e.g., catastrophic perturbation events. Samples of large slow rotating asteroids with shape and spin information is very small because more efforts are needed to obtain enough photometric data to do the shape inversion. Especially, those targets rotating at rates about 1 rev/d or 0.5 rev/day, the coordinated observations of multiple telescopes located at large different longitudes are necessary to determine spin parameters and shape from lightcurves.

For this aim, an a long-term observational project /also a international collaboration was established, in which four Chinese telescopes(an 1.0m telescope at Kunming, a 0.5m at Honghong, and a 0.45m and a 2.4m both at Lijiang site) and four SARA's telescopes(a 0.9m telescope at Kitt Peak, Arizona, U.S.A., and a 0.6m at Cerro Tololo, Chile, an 1.0m at La palma of Canany island, and another 1.0m at campus of butler university, Indiannpolis, U.S.A) were involved now. Here, we presented the succession of observation for asteroids (168) Sibylla and (346) Hermentaria (See Figure 4) in 2014 and 2015 apparitions using telescopes located in China, Chile and USA. Combining previous photometric data and new photometric data, we determined the shape and spin parameters of Sibylla and Hermentaria with the convex inversion method(Kaasalainen & Troppa 2001) and virtual photometry Monte Carlo method (Muinonen et.al 2012). A pair of pole solutions of (168) Sibylla were found around $(4.3°, 53.5°)$ and $(183.5°, 52.6°)$ with a period of 47.0000h. We found the shape of Sibylla is close to an oblate spheroid(Left column of Figure 5). For asteroid (346)

Hermentaria, a pair of pole solutions around (134.5°, 16.7°) and (321.5°, 14.5°) with a comparable RMS values were derived, a spin period of about 17.7900h was derived for the pair of pole, a shape of Hermentaria shows a rough spheroid.(Right column of Figure 5)

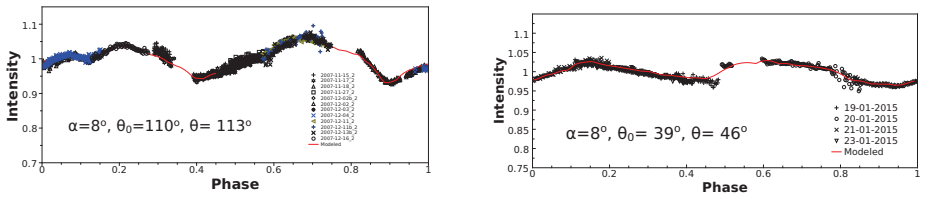

Figure 4. Lightcurves of (168)Sibylla (Left) and (346) Hermentaria (Right).

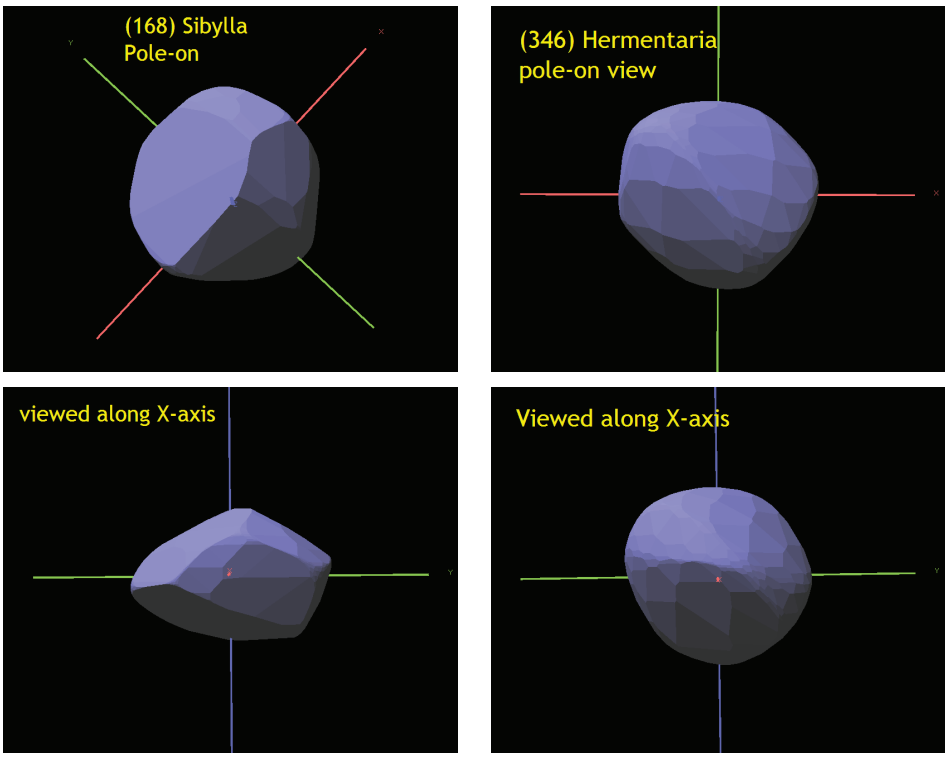

Figure 5. Convex shapes of (168) Sibylla (Left column) and (346) Hermentaria(Right culumn)

4.2. Near Earth asteroid (3200) Phaethon

Near-earth objects, came from main belt asteroids or comets, open a window to us to sight into the small bodies of solar system for their proximity. Therefore, some special near Earth asteroids also our targets to be observed with Lijiang 2.4m telescope.

The apollo-type asteroid (3200) Phaethon has a co-orbit with the Geminid meteor stream, and passes perihelion in a very close distance (about $q = 0.14AU$) each 1.43

year. During each perihelion passages, sub-solar regions on the Phaethon's surface were heated over 1000K. Dust activities of Phaethon had been detected in 2009, 2012, and 2016 by Jewitt (2010a), Li & Jewitt (2013), Jewitt (2013) and Hui&Li (2017). Phaethon is also categorized as 'rocky comet' (Jewitt et al. 2015).

Till now, there were three slight discrepant pole solutions for phaethon: $(97°, -11°)$ given by Krugly et al. (2002), $(90°, -20°)$ by Ansdell et al. (2014), and $(84°, -39°)$ by Hanuš et al. (2016). we carried out the photometric observation for Phaethon in 2015 and 2016. Including existed photometric data of Phaethon, 61 lightcurves of Phaethon were re-analyzed with the convex inversion method and virtual photometry Monta Carlo method. A pair of pole $(98.6°, -25.3°)$ and $(307.7°, -24.9°)$ were derived with a similar RMS. Corresponding to the pair of pole, a very close period of 3.604105 hour was derived. The shape of Phaethon is close to an oblate sphere(See Figure 6). The approximate relative triaxial dimensions of phaethon are a/b = 1.07, b/c =1.24.

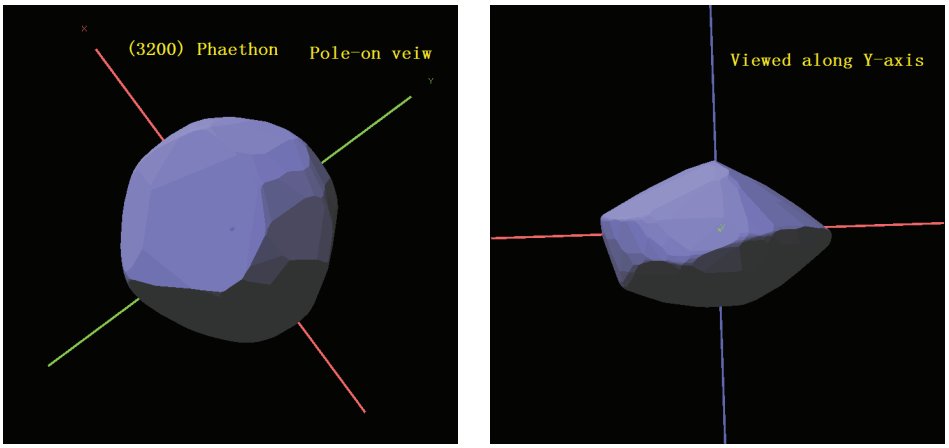

Figure 6. Convex shape of Phaethon

5. Summary and Discussion

1. From brightness and its variations of an asteroid , information on its shape, spin status and photometric phase function can be subtracted based on certain a brightness model. Considering the situation of photometric data obtained and regular or irregular shape of an asteroid, a simple or complicated shape model, is selected during the determination of photometric phase function of asteroids. For case of asteroid (107) Camilla, a ellipsoid shape and Lommel-Seeliger law were involved due to its sine likely lightcurves(see left panel of Figure 1). While a cellinoid shape was used to inverse the phase function of asteroid (106) Dione because of significant asymmetric maximum and minima of lightcurves (see Figure 2).

The characteristics of photometric phase function of asteroids is directly linked to their surface physical properties.Lagerkvist & Magnusson (1990) suggested that the values of slope parameter G in $H - G$ system are distinctly different for the S-, C-, and M-class asteroid. Recent analysis for 93 asteroids' phase functions (Shevchenko et al. 2016) also shown that values of G_1 and G_2 have distinctly regions in $G_1 - G_2$ plot for six main asteroid types: S, M, E, C, D, and P. To some extend, the values of G and/or

G_1 and G_2 can be applied to infer the preliminary type of surface material for those small bodies which is too faint to get spectroscopic data.

Also, we inferred the geometric albedo p for selected asteroids by the values of G_1 and G_2 according to the linear regression relations (Shevchenko et al. 2016): $G_1 = -0.107(\pm0.048)-0.643(\pm0.047)\log(p)$ and $G_2 = 0.644(\pm0.035)+0.433(\pm0.034)\log(p)$. Estimated geometric albedo p of Dione and Camilla are 0.059 and 0.118, respectively, which are consistent with that from IRAS observations (Tedesco et al. 2004) and occultation observations (Shevchenko & Tedesco 2007) in the range of uncertainties of regression parameters.

2. The modeled convex shape of (168) Sibylla is approximately an oblate spheroid with approximate relative axial ratios $a/b = 1.0$ and $b/c = 1.4$, and Hermentaria looks like a spheroid with approximate relative triaxial ratios $a/b = 1.1$ and $b/c = 1.0$. Applying the virtual photometry Monte Carlo method (Muinonen et.al 2012; Wang et al. 2015), we investigated the uncertainties of spin parameters by their distributions which composed of the virtual least-square solutions of the convex inversion. Figure 7 shows distributions of pole of asteroids (168), (346), and (3200). We noted that the degree of dispersion of the distributions is related to photometric errors, number of apparitions of lightcurves and the coverage of phased lightcurve in each apparitions. The smallest dispersion of distribution is that of the slowest rotating asteroid (168) Sibylla for having the most dense data in each features of phased lightcurve. While the largest dispersion occurs in the case of (3200) Phaethon since it has the largest average photometric error (about 0.025 Mag). The uncertainties of pole orientation for two slower rotating asteroids are less than 5 degree, and around 5 degree for Phaethon.

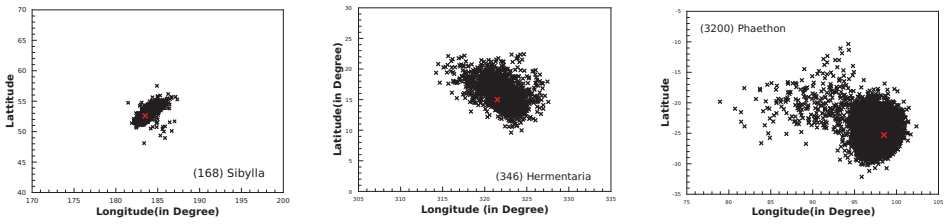

Figure 7. Pole distributions for asteroids 168,346, and 3200

3. During procedure of the shape inversion for Phaethon, we found that three lightcurves (on 2 and 13 Jan. 2016 and 27 Dec. 1997) gave large RMS(see Figure 8), in which remarkable magnitude shifts occur around the repeated part in these three phased lightcurves. Hui&Li (2017) stated that the small-scale activity on Phaethon is due to forward-scattering enhancement at large phase angle. As for the magnitude shifts on three nights, we couldn't explain it with forward-scattering because of its less solar phase angles of 23.4,24.5 and 47.8 degree. We found the latitude of subsolar for observational apparitions in 2016 and 1994 are slight different (52 and 76 degree, respectively). To understand the discrepancy of magnitude in one night, further photometric observations are needed in the next apparition.

Acknowledgments. This work is supported by NSFC through Grant no.11073051 and 11673063 and Academy of Finland(Contract no.127461). We would like to thank management of 2.4m telescope for granting the observation time for the target (3200) Phaethon.

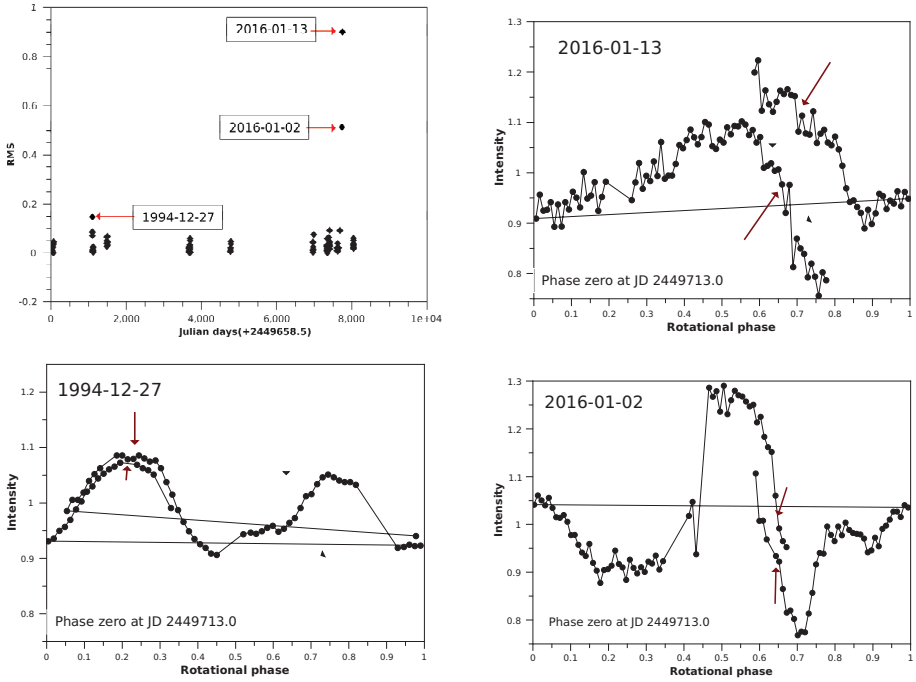

Figure 8. Remarkable deviations of three nights phased lightcurves for Phaethon.

References

Ansdell M., Meech K. J. , Hainaut O., and Buie M. W., 2014,The ApJ, 793,50
Bobrov, M. S., 1970, NASA TT F-701 (Translation of Kol'tsa Saturna, Nauka, Moscow).
Bowell E., and Lumnie K., 1979, In Asteroids (T. Gehrels, Ed.),(Univ, of Arizona Press, 132-169.
Bowell E., Hapke B. , Lumme K., Harris A. W., Domingue D.,and Peltoniemi J., 1989, In Asteroids II, R.P. Binzel, T.Gehrels , M. Matthews, Eds, (Univ, of Arizona Press), 524-556.
Buratti B. J., 1983, Photometric Properties of Europa and the Icy Satellites of Saturn. Ph.D. thesis, Cornell University, Ithaca, New York.
Buratti B. J., 1985, Icarus 61, 208-217.
Cellino A., Zappala V.,& Farinella P., 1989, Icarus 78, 298.
Dymock R., & Miles R. 2009, Journal of the British Astronomical Association, 119, 149, 5
Esposito L. W., 1979, Icarus, 39, 69.
Hapke B., 1963, Astronomical Journal, 68, 279-280.
Hapke B., 2012, Theory of reflectance and meittance spectroscopy, second edition, Cambridge university press
Hanuš J., Delbo M., VokrouhlickýD., Pravec P., Emery J. P., Alĺ-Lagoa V. , Bolin B., Devogeèle M., Dyvig R., Gálád A., Jedicke R., KornošL., Kušnirák P., Licandro J., Reddy V., Rivet J.-P., Vila´gi J., and Warner B. D., 2016, A&A 592, A34
Hui M.-T. & Li J., 2017, AJ, 153,23
Irvine W. M., 1966, Astronomical Journal, Vol. 71, 859.
Jewitt D., & Li J. 2010, AJ, 140, 1519
Jewitt D., Li J., & Agarwal J. 2013, ApJL, 771, L36
Jewitt D. 2013, AJ, 145, 133

Jewitt D., Hsieh H., & Agarwal J. 2015, in Asteroids IV, ed. P. Michel, F. DeMeo, & W. Bottke (Tucson, AZ: Univ. Arizona Press), 221
Kaasalainen M. & Torppa J., 2001, Icarus, 153, 24
Kaasalainen M., Torppa J., & Muinonen K. 2001, Icarus, 153, 37
Kaasalainen M., Torppa J., & Piironen J. 2002, Icarus, 159,369
Krugly Y. N., Belskaya I. N., Shevchenko V. G., et al. 2002, Icar, 158, 294
Lambert J. H., 1760, Photometria, sive de Mensura et gradibus luminis, colorum et umbrae.
Lagerkvist C.-I. & Magnusson P.,1990, A&AS, 86, 119L
Li J.-Y., A'Hearn M. F., & McFadden L. A., 2004, Icarus 172, 415-431.
Li J.-Y., 2015, Asteroids IV, (Tucson, AZ: Univ. Arizona Press), 129-150,
Li J., & Jewitt D. 2013, AJ, 145,154
Lumme K., 1970, Astrophys. Space Sci. 8, 90-101.
Lumme K., & Bowell E., 1981, Astron. J. 86, 1694-1704.
Lumme K., & Bowell E., 1981, Astron. J. 86, 1705-1712.
Lumme K., Muinonen K., Peltoniemi J., Karttunen H., & Bowell E., 1987 , Bull. Am. Astron. Soc. 19,850.
Minnaert M., 1941, Astrophys. J., 93,403-410
Mishchenko M., Dlugach J. M., 1993, P&SS, 41, no. 3, 173-181.
Muinonen K., 1989 , In Proc. 1989, URSI Electromagnetic Theory Symposium, 428-430, Stockholm, Sweden.
Muinonen K., Belskaya I., Cellino A., Delbo M., Levasseur-Regourd A.-C., Penttila A., TedescoE., 2010, Icarus 209, 542-555.
Muinonen K., Granvik M., Oszkiewicz D., Pieniluoma T., & Pentikäinen H. 2012, P&SS, 73, 15.
Muinonen K., Wilkman O., Cellino A., Wang X., & Wang Y., 2015, P&SS, 118,227-241
Müller, G., 1893, Publ. Astrophys. Obs. Potsdam, 30, 198-389.
Von Seeliger H., 1887, Abh. Bayer. Akad. Wiss. Math. Naturwiss. Kl. 16, 405-516.
Shevchenko V. G. & Tedesco E. F., Asteroid Albedos from Stellar Occultations V1.0 EAR-A-VARGBDET-5-OCCALB-V1.0. NASA Planetary Data syatem,2007 .
Shevchenko V.G. & Tedesco E.F., 2007, Asteroid Albedos from Stellar Occultations V1.0, EAR-A-VARGBDET-5-OCCALB-V1.0, NASA Planetary Data System
Shevchenko V. G., Belskaya I. N., Muinonen K., Penttilä A., Krugly Y. N., Velichko F. P., Chiorny V. G., Slyusarev Ivan G., Gaftonyuk N. M., & Tereschenko, I. A., 2016, P&SS, 123, 101S
Shkuratov Yu. G., 1985, Circular No.1400, 3-6
Tedesco E. F., Noah P.V., Noah M. & Price S.D., 2004, IRAS minor planets survey, IRAS-A-FPA-3-RDR-IMPS-V6.0, NASA Planetary Data syatem.
Wang X.B., Muinonen K., Wang Y.B., Behrend R., Goncalves R., Oey J., Antonini P.,Demeautis C., Manzini F., Damerdji J., Montier J., Klotz A., Leroy A., & Ganand G.,2015, A&A 581, A55
Wang Y. B., Wang X.B., & A. Wang, 2016, RAA Vol. 16, No. 9
Wang Y. B., Wang X.B., Pray P., & Wang A. 2017, RAA, in press
Wilkman O., Muinonen K., & Peltoniemi J., 2015, P&SS,118,250

Prof. Xiaobin Wang wishing Prof. Ip a wonderful birthday and many sunny days.